



Dynamics of an open double quantum dot system via quantum measurementKang Lan, Qian Du, Lisha Kang, Xu Tang, Lujing Jiang, and Yanhui Zhang ^{*}
*School of Physics and Electronics, Shandong Normal University, Jinan 250014, China*Xiangji Cai ^{*}*School of Science, Shandong Jianzhu University, Jinan 250101, China*

(Received 9 April 2019; revised manuscript received 17 September 2019; accepted 13 April 2020; published 4 May 2020)

We study the dynamics of a double quantum dot (DQD) system interacting with a Gaussian white noise (GWN) environment which is measured by a quantum point contact (QPC) device. With both the transverse and longitudinal noise taken into account, we utilize an effective method by adding an additional Bloch vector to calculate the cumulant generating functions of the electron transfer in the QPC detector based on the full counting statistics. We study the average detector current, Fano factor, and average waiting time of the electron transfer in the presence of decoherence effects of the DQD system caused by both the QPC and the GWN environment. It indicates that the decoherence effects arising from the QPC and the GWN environment have obviously different influences on the electron transfer detected by the QPC device in both short-time and long-time limits. It is shown that the measurement process would localize the electron in a DQD in a short time and that the distribution of the average current and Fano factor versus level displacement in long-time limit are broadened due to the interaction between the system and GWN environment, which provides a reliable method to explore the dynamical behavior of an open quantum system and to extract the characteristics of the environment by analyzing the detector outcome. Our results provide theoretical support for studies of quantum measurement in a semiconductor device affected by a fluctuant environment.

DOI: [10.1103/PhysRevB.101.174302](https://doi.org/10.1103/PhysRevB.101.174302)**I. INTRODUCTION**

Quantum measurement, which is the basis of understanding the origin of decoherence and realizing quantum coherent control in quantum information science, has always been a hot research topic in the microscopic field [1–12]. It is still an urgent problem and of abundant value to explore the decoherence mechanism caused by the interaction between the quantum system and its environments. To better detect the decoherence processes induced by its environments, it is necessary to relate the detector outcome to the dynamical behavior of open quantum systems [13–16]. Recently, the non-Markovian dynamics of open quantum systems has drawn much attention due to its important role in the community of quantum physics [17–30], which has promoted a wide range of applications in many excellent theoretical research areas [31–35].

The double quantum dot (DQD) system provides a perfect model for us to study the dynamical properties via quantum measurement [15,36–48]. The quantum point contact (QPC) device has been widely used as the main detector for measurements of dynamical behavior in DQD systems. Many useful dynamical properties of the open DQD system can be obtained by analyzing the cumulants of the number of

transferred electrons detected by the QPC device [46,47]. The method of full counting statistics (FCS) has been widely used to clarify the distribution of the number of transferred electrons. Recently, the first and second cumulants, related to the average current and shot noise, respectively, were studied as meaningful research objects induced by the interaction between the system and its environments in the transport process [49–51]. Another important physical quantity, the Fano factor, can be identified numerically to $F = 1$, $F < 1$, and $F > 1$, which correspond to the Poissonian, sub-Poissonian, and super-Poissonian distributions for the shot noise.

It is very important to indicate the dynamical behavior of an open quantum system and the characteristics of the environment by analyzing the detector outcome. The noise spectrum is the indicator of the current fluctuations, which can effectively show the dynamical characteristics of the system influenced by the environmental noise [7,13,37,52]. Especially, the nonzero higher-order cumulants can characterize the non-Gaussian behavior of the system dynamics [53]. However, the short-time dynamical information of the system may be lost via the method of FCS, which characterizes the number of transferred particles in the long-time limit [54]. To describe the crucial short-time dynamical information with rapid detection, it is necessary to study the average waiting time of the electron transfer in the detector device [35,54,55].

In general, the decoherence of the quantum system induced by the environmental effects displays in two different ways: relaxation and dephasing [5,15,47,56,57]. Quantum

^{*}Corresponding authors: yhzhang@sdnu.edu.cn;
xiangjicai@foxmail.com

measurements of the DQD system coupled to its environments with constant relaxation and dephasing rates have been well studied by means of a QPC device as a detector [13,15,37]. However, the relaxation and dephasing rates induced by the environments may not always be constant but time dependent. In this situation, the effects of the environments on the quantum system can be better described by stochastic environmental noise, which provides profound insights to study quantum decoherence, geometric phases [28,58], dynamical decoupling [59,60], etc. Gaussian white noise (GWN) of a stationary Ornstein-Uhlenbeck (OU) type has been widely used to study and simulate the effect of the environments on the open quantum system dynamics with time-dependent decoherence rate [59,61]. Thus, it is very useful and effective to study the quantum measurement of a DQD system in the presence of a GWN environment by a QPC detector.

In this paper, we consider the dynamical properties of a DQD system interacting with a stochastically fluctuating GWN environment via quantum measurement detected by a QPC device. The dynamical evolution of the reduced density matrix of the open DQD system is governed by a time-convolutionless master equation. By adding an additional vector to the Bloch vectors, we accurately calculate the detector average current, the Fano factor, and the average waiting time, which display the dynamical properties of the DQD system and the characteristics of the environment. The Fano factor always follows the super-Poissonian distribution, which can be attributed to the cotunneling and the quantum coherence. It is shown that the GWN parameters have a broadening behavior on the distributions of average current and Fano factor. Moreover, the Fano factor showed a higher sensitivity to GWN than the average current for the small level displacement. Additionally, the increase of the average waiting time caused by the coupling between the DQD system and QPC proves that frequent measurements enhance localization of the electron in the short time. Our research not only reveals the dynamical properties in the GWN environment but also provides a theoretical reference for the development of quantum measurement theory.

This paper is organized as follows. In Sec. II, we describe the measurement of a DQD by a QPC in the GWN environment and derive the dynamical evolution equation of the system. On this basis, we give the n -resolved density matrix associated with the number of transferred electrons. In Sec. III, we obtain the cumulant generating function of electrons from the methods of the FCS and an additional Bloch vector. In Sec. IV, we study the average current, the Fano factor, and the average waiting time of the detector in the open DQD system and discuss the dynamical significance of these physical quantities, respectively. In Sec. V, we give the conclusions of this paper.

II. THEORETICAL FRAMEWORK

We begin by considering a DQD system weakly detected by a QPC device, as shown in Fig. 1. The basis of the system can be denoted by $|L\rangle$ and $|R\rangle$, representing an electron localized in the left or right dots, respectively. The Hamiltonian of

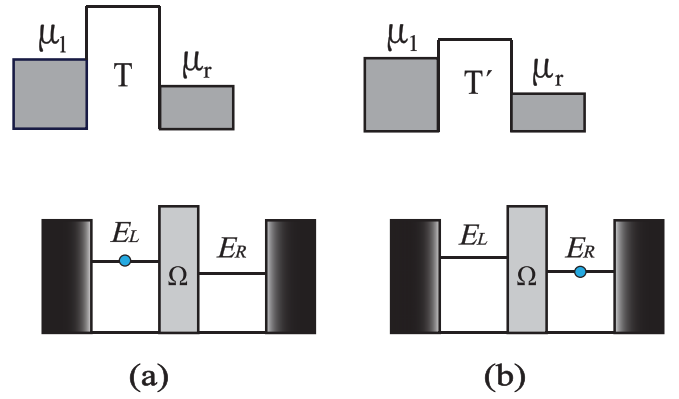


FIG. 1. A double quantum dot two-level system and a QPC detector; E_L and E_R are the energy levels of the left and right quantum dots, respectively. $\mu_{l,r}$ denote the chemical potentials in the left and right reservoirs, and $V = \mu_l - \mu_r$ is the bias voltage. T and T' represent the transparency in the QPC detector for an electron localized in the left or right dot.

the whole system can be described as

$$H = H_0 + H_{PC} + H_I, \quad (1)$$

where H_0 , H_{PC} , and H_I are, respectively, the Hamiltonians of the DQD, the QPC, and the interaction between the DQD and QPC [13]:

$$\begin{aligned} H_0 &= \frac{\hbar}{2}(\Delta_0\sigma_z + \Omega_0\sigma_x), \\ H_{PC} &= \sum_l E_l a_l^\dagger a_l + \sum_r E_r a_r^\dagger a_r + \sum_{l,r} (T a_r^\dagger a_l + \text{H.c.}), \\ H_I &= \sum_{l,r} \delta T \sigma_z (a_r^\dagger a_l + a_l^\dagger a_r). \end{aligned} \quad (2)$$

Here σ_z and σ_x denote the Pauli matrices in terms of the basis $\{|L\rangle, |R\rangle\}$, and Δ_0 and Ω_0 refer to the level displacement and stationary coupling of the DQD. E_l and E_r are quantum states in the left and right reservoirs of the detector, and a_l^\dagger (a_l) and a_r^\dagger (a_r) are the creation (annihilation) operators of the left and right reservoirs in the QPC [13,15]; $\delta T = T - T'$ depends on which dot of the DQD system is occupied by the electron [5]. We assume that the transparency is weakly dependent on states l, r in the detector. Thus, it can be represented by its average value, namely, $T = T_0$ and $T' = T_0 - \delta T_0$.

We consider the DQD system to simultaneously interact with a stochastically fluctuating environment. The environmental effect on the quantum system could be described by means of stochastic fluctuations in some system observable based on the Kubo-Anderson spectral diffusion process [62–64]. Due to the environmental effect, the stochastic fluctuations in the Hamiltonian of the DQD system can be written as

$$H(t) = H_0 + H_\delta(t) = \frac{\hbar}{2}[\Delta(t)\sigma_z + \Omega(t)\sigma_x], \quad (3)$$

where the energy difference $\Delta(t)$ and coupling strength $\Omega(t)$ of the two-level system fluctuate stochastically as

$$\Delta(t) = \Delta_0 + \delta\Delta(t), \quad \Omega(t) = \Omega_0 + \delta\Omega(t). \quad (4)$$

Here $\delta\Delta(t)$ and $\delta\Omega(t)$ are the longitudinal noise and transverse noise of the system induced by the environment, respectively [58].

By tracing out the QPC detector and taking the average over the environmental noise, the dynamical evolution of the reduced density matrix of the system $\rho(t)$ generally satisfies a generalized master equation [65]. The reduced density matrix can be resolved to $\rho(t) = \sum_{n=0}^{\infty} \rho^{(n)}(t)$, with the component $\rho^{(n)}(t)$ associated with the number of transferred electrons n . The n -resolved density matrix of the system is formally governed by a generalized master equation as [33,34]

$$\frac{d}{dt}\rho^{(n)}(t) = \sum_{n'} \int_0^t dt' \mathcal{W}(n-n', t-t') \rho^{(n')}(t') + \gamma(n, t), \quad (5)$$

where the memory kernel $\mathcal{W}(\Delta n, dt)$ accounts for the influence of both the detector and environmental noise on the dynamical evolution of the system and $\gamma(n, t)$ describes the correlations induced by the detector and environmental noise initially. The memory effect and initial correlations vanish when the memory kernel $\mathcal{W}(\Delta n, dt)$ is proportional to a δ function and there are no initial correlations between the system and the detector and environmental noise, respectively.

In the following, we derive the dynamical evolution of the reduced density matrix of the system weakly detected by a QPC device and coupled to a GWN environment. We consider a general case in which the fluctuation noises in the longitudinal and transverse directions are both GWN of a stationary OU type and independent of each other. First, we consider that the DQD system is only weakly coupled to the QPC detector. In the limit in which a large bias voltage applies to the QPC device, namely, $eV \gg T_0\rho_d$, where ρ_d is the density of states in the reservoir of the QPC, the effect of the detector leads to the decay of the off-diagonal elements of the reduced density matrix, and the dynamical evolution of the reduced density matrix satisfies

$$\frac{d}{dt}\rho(t) = L_0\rho(t) + L_d\rho(t), \quad (6)$$

where $L_0\rho(t) = -\frac{i}{\hbar}[H_0, \rho(t)]$ is the Liouville operator that describes the unitary evolution of the system and L_d describes the decoherence caused by the QPC detector with the decoherence rate $\Gamma_d = D + D' - 2\sqrt{DD'}$, where $D = T(\mu_l - \mu_r)/2\pi$ is the rate of electron hopping from the left to the right reservoir [5]. Using a column vector representation for the reduced density matrix of the system

$$\rho(t) = [\rho_{LL}(t), \rho_{RR}(t), \rho_{RL}(t), \rho_{LR}(t)]^\dagger, \quad (7)$$

the operators L_0 and L_d can be respectively written as

$$L_0 = \begin{pmatrix} 0 & 0 & i\frac{\Omega_0}{2} & -i\frac{\Omega_0}{2} \\ 0 & 0 & -i\frac{\Omega_0}{2} & i\frac{\Omega_0}{2} \\ i\frac{\Omega_0}{2} & -i\frac{\Omega_0}{2} & -i\Delta_0 & 0 \\ -i\frac{\Omega_0}{2} & i\frac{\Omega_0}{2} & 0 & i\Delta_0 \end{pmatrix}, \quad (8)$$

$$L_d = \begin{pmatrix} 0 & 0 & 0 & 0 \\ 0 & 0 & 0 & 0 \\ 0 & 0 & -\frac{\Gamma_d}{2} & 0 \\ 0 & 0 & 0 & -\frac{\Gamma_d}{2} \end{pmatrix}.$$

The time evolution for the n -resolved density matrix can be derived within the Born-Markov approximation as [66]

$$\frac{d}{dt}\rho^{(n)}(t) = L\rho^{(n)}(t) + L_J\rho^{(n-1)}(t), \quad (9)$$

where L and L_J respectively describe the continuous evolution of the system and the quantum jumps of the electron transfer to the collector. The corresponding operators L and L_J can be expressed as

$$L = \begin{pmatrix} -D & 0 & i\frac{\Omega_0}{2} & -i\frac{\Omega_0}{2} \\ 0 & -D' & -i\frac{\Omega_0}{2} & i\frac{\Omega_0}{2} \\ i\frac{\Omega_0}{2} & -i\frac{\Omega_0}{2} & -i\Delta_0 - \frac{D+D'}{2} & 0 \\ -i\frac{\Omega_0}{2} & i\frac{\Omega_0}{2} & 0 & i\Delta_0 - \frac{D+D'}{2} \end{pmatrix},$$

$$L_J = \begin{pmatrix} D & 0 & 0 & 0 \\ 0 & D' & 0 & 0 \\ 0 & 0 & \sqrt{DD'} & 0 \\ 0 & 0 & 0 & \sqrt{DD'} \end{pmatrix}. \quad (10)$$

The n -resolved density matrix within the Born-Markov approximation in Eq. (9) is a special case of Eq. (5) with no memory effect and an initial correlation between the DQD system and QPC device.

Now, we consider that the system interacts only with the GWN environment and assume there is no coupling between the DQD and the QPC detector. The Hamiltonian in Eq. (3) can be divided into two parts as

$$H(t) = H_0 + H_\delta(t) = \frac{\hbar}{2}(\Delta_0\sigma_z + \Omega_0\sigma_x) + \frac{\hbar}{2}[\delta\Delta(t)\sigma_z + \delta\Omega(t)\sigma_x], \quad (11)$$

where H_0 is the intrinsic Hamiltonian of the DQD system and $H_\delta(t)$ is the fluctuation term caused by the longitudinal and transverse noises coupled to the DQD system. The statistical properties of the longitudinal and transverse OU-type GWN are described by the correlation functions

$$\langle \delta\Delta(t)\delta\Delta(t') \rangle_\delta = \sigma_\Delta^2 e^{-\tau_\Delta(t-t')},$$

$$\langle \delta\Omega(t)\delta\Omega(t') \rangle_\delta = \sigma_\Omega^2 e^{-\tau_\Omega(t-t')}, \quad (12)$$

where σ_Ω and σ_Δ are the amplitudes of the noise in the transverse and longitudinal directions, respectively, and τ_Ω and τ_Δ are the damping coefficients.

The dynamical evolution for the reduced density matrix $\rho(t)$ of the open DQD system can be determined by taking an ensemble average over the environmental noise as $\rho(t) = \langle \rho(t; \delta(t)) \rangle_\delta$, with $\rho(t; \delta(t))$ being the total density matrix depending on the GWN. The evolution of the total density matrix yields the Liouville equation,

$$\frac{\partial}{\partial t}\rho(t; \delta(t)) = [L_0 + L_\delta(t)]\rho(t; \delta(t)), \quad (13)$$

where the superoperator $L_\delta(t)\rho(t) = -\frac{i}{\hbar}[H_\delta(t), \rho(t)]$ describes the fluctuation effect of the environmental noise on the density matrix. Using the representation for the reduced

density matrix in Eq. (7), the operator $L_\delta(t)$ can be written as

$$L_\delta(t) = \begin{pmatrix} 0 & 0 & i\frac{\delta\Omega(t)}{2} & -i\frac{\delta\Omega(t)}{2} \\ 0 & 0 & -i\frac{\delta\Omega(t)}{2} & i\frac{\delta\Omega(t)}{2} \\ i\frac{\delta\Omega(t)}{2} & -i\frac{\delta\Omega(t)}{2} & -i\delta\Delta(t) & 0 \\ -i\frac{\delta\Omega(t)}{2} & i\frac{\delta\Omega(t)}{2} & 0 & i\delta\Delta(t) \end{pmatrix}. \quad (14)$$

In the presence of a general environment, the dynamical evolution of the reduced density matrix formally follows two types of equations, namely, time-convolution and time-convolutionless quantum master equations, as derived in Appendix A. In a GWN environment, based on the statistical

property of the noise and taking an ensemble average over the environmental noise, the dynamical evolution of the system is governed by a time-convolutionless master equation as (see Appendix A)

$$\frac{d}{dt}\rho(t) = L_0\rho(t) + \int_0^t dt' \langle L_\delta(t) e^{L_0(t-t')} L_\delta(t') \rangle_\delta e^{-L_0(t-t')} \rho(t'). \quad (15)$$

Such a dynamical equation (15) is exact for an environment with a GWN statistical property. In terms of the operators L_0 and $L_\delta(t)$ expressed above, the evolution of the elements of the reduced density matrix in Eq. (15) can be written as (see Appendix B)

$$\begin{aligned} \dot{\rho}_{LL}(t) &= -\Omega_0 \left\{ \frac{i}{2} + \frac{\Delta_0 \sigma_\Omega^2}{2\Omega_L^2} \left[\frac{1}{(\tau_\Omega^2 + \Omega_L^2)} [\tau_\Omega - e^{-\tau_\Omega t} \tau_\Omega \cos(\Omega_L t) + \Omega_L e^{-\tau_\Omega t} \sin(\Omega_L t)] - \frac{(1 - e^{-\tau_\Omega t})}{\tau_\Omega} \right] \right\} \rho_{RL}(t) \\ &+ \Omega_0 \left\{ \frac{i}{2} - \frac{\Delta_0 \sigma_\Omega^2}{2\Omega_L^2} \left[\frac{1}{(\tau_\Omega^2 + \Omega_L^2)} [\tau_\Omega - e^{-\tau_\Omega t} \tau_\Omega \cos(\Omega_L t) + \Omega_L e^{-\tau_\Omega t} \sin(\Omega_L t)] + \frac{(1 - e^{-\tau_\Omega t})}{\tau_\Omega} \right] \right\} \rho_{LR}(t) \\ &- \frac{\sigma_\Omega^2}{2\Omega_L^2} \left[\frac{\Delta_0^2}{(\tau_\Omega^2 + \Omega_L^2)} [\tau_\Omega - e^{-\tau_\Omega t} \tau_\Omega \cos(\Omega_L t) + \Omega_L e^{-\tau_\Omega t} \sin(\Omega_L t)] + \frac{\Omega_0^2}{\tau_\Omega} (1 - e^{-\tau_\Omega t}) \right] [\rho_{LL}(t) - \rho_{RR}(t)], \\ \dot{\rho}_{RL}(t) &= \left[-i\frac{\Omega_0}{2} - i\frac{\Omega_0 \sigma_\Delta^2}{2\Omega_L(\tau_\Delta^2 + \Omega_L^2)} [\Omega_L - \tau_\Delta e^{-\tau_\Delta t} \sin(\Omega_L t) - \Omega_L e^{-\tau_\Delta t} \cos(\Omega_L t)] \right. \\ &- \frac{\Omega_0 \Delta_0 \sigma_\Delta^2}{2\Omega_L(\tau_\Delta^2 + \Omega_L^2)} [\tau_\Delta - e^{-\tau_\Delta t} \tau_\Delta \cos(\Omega_L t) + e^{-\tau_\Delta t} \Omega_L \sin(\Omega_L t)] + \frac{\Delta_0 \Omega_0 \sigma_\Delta^2}{2\Omega_L^2 \tau_\Delta} (1 - e^{-\tau_\Delta t}) \left. \right] [\rho_{LL}(t) - \rho_{RR}(t)] \\ &- \left[\frac{\Omega_0^2 \sigma_\Omega^2}{2\tau_\Omega \Omega_L^2} (1 - e^{-\tau_\Omega t}) + \frac{\Delta_0^2 \sigma_\Omega^2}{2\Omega_L^2 (\tau_\Omega^2 + \Omega_L^2)} [\tau_\Omega - e^{-\tau_\Omega t} \tau_\Omega \cos(\Omega_L t) + \Omega_L e^{-\tau_\Omega t} \sin(\Omega_L t)] \right] [\rho_{RL}(t) - \rho_{LR}(t)] \\ &+ \frac{i\Delta_0 \sigma_\Omega^2}{2\Omega_L(\tau_\Omega^2 + \Omega_L^2)} [\Omega_L - \tau_\Omega e^{-\tau_\Omega t} \sin(\Omega_L t) - \Omega_L e^{-\tau_\Omega t} \cos(\Omega_L t)] [\rho_{RL}(t) + \rho_{LR}(t)] \\ &+ \left[i\Delta_0 - \frac{\Delta_0^2 \sigma_\Delta^2}{\Omega_L^2 \tau_\Delta} (1 - e^{-\tau_\Delta t}) - \frac{\Omega_0^2 \sigma_\Delta^2}{\Omega_L^2 (\tau_\Delta^2 + \Omega_L^2)} [\tau_\Delta - e^{-\tau_\Delta t} \tau_\Delta \cos(\Omega_L t) + e^{-\tau_\Delta t} \Omega_L \sin(\Omega_L t)] \right] \rho_{RL}(t), \quad (16) \end{aligned}$$

where $\rho_{RR}(t) = 1 - \rho_{LL}(t)$, $\rho_{LR}(t) = \rho_{RL}^*(t)$, and $\Omega_L^2 = \Delta_0^2 + \Omega_0^2$. The diagonal terms $\rho_{LL}(t)$ and $\rho_{RR}(t)$ are the probabilities of finding the electron in the left and right dots, respectively. The off-diagonal terms $\rho_{LR}(t)$ and $\rho_{RL}(t)$ describe the coherences between states $|L\rangle$ and $|R\rangle$.

Considering the QPC detector is large voltage biased, both the couplings between the system and QPC device and between the system and the GWN environment are very weak. Based on the methods used in Refs. [4,5], we can derive the dynamical evolution of the reduced density matrix in the presence of both the QPC detector and the GWN environment as

$$\begin{aligned} \frac{d}{dt}\rho(t) &= L_0\rho(t) + L_d\rho(t) \\ &+ \int_0^t dt' \langle L_\delta(t) e^{L_0(t-t')} L_\delta(t') \rangle_\delta e^{-L_0(t-t')} \rho(t'), \quad (17) \end{aligned}$$

where the first term on the right-hand side describes the unitary evolution of the system, the second term represents the decoherence induced by the QPC detector, and the third

term is the influence caused by the GWN environment. The form of the dynamical evolution of the reduced density matrix in Eq. (17) is consistent with that derived by second-order cumulant expansion for the case of a non-Gaussian Markovian environment [36,37,40].

As a consequence, the n -resolved density matrix associated with the number of transferred electrons is governed by

$$\begin{aligned} \frac{d}{dt}\rho^{(n)}(t) &= L\rho^{(n)}(t) + L_J\rho^{(n-1)}(t) \\ &+ \int_0^t dt' \langle L_\delta(t) e^{L_0(t-t')} L_\delta(t') \rangle_\delta e^{-L_0(t-t')} \rho^{(n)}(t') \end{aligned} \quad (18)$$

in terms of the operators defined in Eqs. (8), (10), and (14).

III. ADDITIONAL BLOCH VECTOR AND FULL COUNTING STATISTICS

We relate the n -resolved density matrix to the physical quantities detected by the QPC via the cumulant generating

function as [15]

$$\rho(x, t) = \sum_{n=0}^{\infty} \rho^{(n)}(t) e^{-nx}, \quad (19)$$

where x is the extra factor to manifest the counting parameter of the electrons.

In order to study the dynamical properties of the system more conveniently, we introduce the Bloch vectors and an additional vector to simplify the calculations [15,67],

$$\begin{aligned} \mathcal{U}(x, t) &= \rho_{LR}(x, t) + \rho_{RL}(x, t), \\ \mathcal{V}(x, t) &= \frac{1}{i} [\rho_{LR}(x, t) - \rho_{RL}(x, t)], \\ \mathcal{W}(x, t) &= \rho_{LL}(x, t) - \rho_{RR}(x, t). \end{aligned} \quad (20)$$

The additional Bloch vector is

$$\mathcal{Y}(x, t) = \rho_{LL}(x, t) + \rho_{RR}(x, t), \quad (21)$$

which makes it more convenient to obtain the statistical information of the number of transfer electrons in the detector.

It is easy to acquire these new Bloch-type differential equations for the generating functions,

$$\begin{aligned} \dot{\mathcal{U}}(x, t) &= \left[-\frac{\Omega_0 \Delta_0 \sigma_{\Delta}^2}{\Omega_L^2 (\tau_{\Delta}^2 + \Omega_L^2)} [\tau_{\Delta} - e^{-\tau_{\Delta} t} \tau_{\Delta} \cos(\Omega_L t) + e^{-\tau_{\Delta} t} \Omega_L \sin(\Omega_L t)] + \frac{\Delta_0 \Omega_0 \sigma_{\Delta}^2}{\Omega_L^2 \tau_{\Delta}} (1 - e^{-\tau_{\Delta} t}) \right] \mathcal{W}(x, t) \\ &\quad - \left[\frac{\Delta_0^2 \sigma_{\Delta}^2}{\Omega_L^2 \tau_{\Delta}} (1 - e^{-\tau_{\Delta} t}) + \frac{\Omega_0^2 \sigma_{\Delta}^2}{\Omega_L^2 (\tau_{\Delta}^2 + \Omega_L^2)} [\tau_{\Delta} - e^{-\tau_{\Delta} t} \tau_{\Delta} \cos(\Omega_L t) + e^{-\tau_{\Delta} t} \Omega_L \sin(\Omega_L t)] \right] \mathcal{U}(x, t) \\ &\quad + \Delta_0 \mathcal{V}(x, t) + \left[\sqrt{DD'} e^{-x} - \frac{D + D'}{2} \right] \mathcal{U}(x, t), \\ \dot{\mathcal{V}}(x, t) &= \left[\Omega_0 + \frac{\Omega_0 \sigma_{\Delta}^2}{\Omega_L (\tau_{\Delta}^2 + \Omega_L^2)} [\Omega_L - \tau_{\Delta} e^{-\tau_{\Delta} t} \sin(\Omega_L t) - \Omega_L e^{-\tau_{\Delta} t} \cos(\Omega_L t)] \right] \mathcal{W}(x, t) \\ &\quad - \left[\frac{\Delta_0 \sigma_{\Omega}^2}{\Omega_L (\tau_{\Omega}^2 + \Omega_L^2)} [\Omega_L - \tau_{\Omega} e^{-\tau_{\Omega} t} \sin(\Omega_L t) - \Omega_L e^{-\tau_{\Omega} t} \cos(\Omega_L t)] + \Delta_0 \right] \mathcal{U}(x, t) \\ &\quad - \left[\frac{\Omega_0^2 \sigma_{\Omega}^2}{\Omega_L^2 \tau_{\Omega}} (1 - e^{-\tau_{\Omega} t}) + \frac{\Delta_0^2 \sigma_{\Omega}^2}{\Omega_L^2 (\tau_{\Omega}^2 + \Omega_L^2)} [\tau_{\Omega} - e^{-\tau_{\Omega} t} \tau_{\Omega} \cos(\Omega_L t) + \Omega_L e^{-\tau_{\Omega} t} \sin(\Omega_L t)] \right] \mathcal{V}(x, t) \\ &\quad - \left[\frac{\Delta_0^2 \sigma_{\Delta}^2}{\Omega_L^2 \tau_{\Delta}} (1 - e^{-\tau_{\Delta} t}) + \frac{\Omega_0^2 \sigma_{\Delta}^2}{\Omega_L^2 (\tau_{\Delta}^2 + \Omega_L^2)} [\tau_{\Delta} - e^{-\tau_{\Delta} t} \tau_{\Delta} \cos(\Omega_L t) + \Omega_L e^{-\tau_{\Delta} t} \sin(\Omega_L t)] \right] \mathcal{V}(x, t) \\ &\quad - \left[\frac{D + D'}{2} - \sqrt{DD'} e^{-x} \right] \mathcal{V}(x, t), \\ \dot{\mathcal{W}}(x, t) &= -\Omega_0 \mathcal{V}(x, t) - \left[\frac{\Omega_0 \Delta_0 \sigma_{\Omega}^2}{\Omega_L^2 (\tau_{\Omega}^2 + \Omega_L^2)} [\tau_{\Omega} - e^{-\tau_{\Omega} t} \tau_{\Omega} \cos(\Omega_L t) + \Omega_L e^{-\tau_{\Omega} t} \sin(\Omega_L t)] - \frac{\Omega_0 \Delta_0 \sigma_{\Omega}^2}{\Omega_L^2 \tau_{\Omega}} (1 - e^{-\tau_{\Omega} t}) \right] \mathcal{U}(x, t) \\ &\quad - \frac{\sigma_{\Omega}^2}{\Omega_L^2} \left[\frac{\Delta_0^2}{(\tau_{\Omega}^2 + \Omega_L^2)} [\tau_{\Omega} - e^{-\tau_{\Omega} t} \tau_{\Omega} \cos(\Omega_L t) + \Omega_L e^{-\tau_{\Omega} t} \sin(\Omega_L t)] + \frac{\Omega_0^2}{\tau_{\Omega}} (1 - e^{-\tau_{\Omega} t}) \right] \mathcal{W}(x, t) \\ &\quad - \frac{(1 - e^{-x})(D + D')}{2} \mathcal{W}(x, t) - \frac{(1 - e^{-x})(D - D')}{2} \mathcal{Y}(x, t), \\ \dot{\mathcal{Y}}(x, t) &= \left[-\frac{D(1 - e^{-x})}{2} + \frac{D'(1 - e^{-x})}{2} \right] \mathcal{W}(x, t) - \left[\frac{D(1 - e^{-x})}{2} + \frac{D'(1 - e^{-x})}{2} \right] \mathcal{Y}(x, t). \end{aligned} \quad (22)$$

We discuss the statistical information in the transfer process by differentiating $\mathcal{Y}(x, t)$ with respect to x . The cumulant generating function of electrons from the additional Bloch vector can be written as

$$\langle N^{(k)} \rangle = (-1)^k \frac{\partial^k}{\partial x^k} \mathcal{Y}(x, t) |_{x=0}. \quad (23)$$

The probability of n electrons transferred during the t interval is

$$P_n(t) = (-1)^n \frac{\partial^n}{\partial x^n} \mathcal{Y}(x, t) |_{x=\infty}. \quad (24)$$

The average detector current is given by $I(t) = e \frac{d\langle N \rangle}{dt}$, and $\langle N \rangle$ is the average number of electrons that have arrived in the

right reservoir. We set the charge of the electron as $e = 1$, so the average detector current can be written as

$$I(t) = \langle \dot{N} \rangle = -\frac{\partial}{\partial x} \dot{Y}(x, t)|_{x=0}. \quad (25)$$

In order to describe the dynamics of the electron transport in more detail, we calculate the Fano factor to characterize the distribution of the shot noise

$$F = \frac{\langle N^2 \rangle - \langle N \rangle^2}{\langle N \rangle}. \quad (26)$$

Meanwhile, the crucial short-time dynamical information, namely, the average waiting time, is determined by [54]

$$\langle \tau \rangle = \int_0^\infty P_0(t) dt. \quad (27)$$

IV. DYNAMICS OF AN OPEN DOUBLE QUANTUM DOT SYSTEM

In this section, we show the numerical results of the physical quantities detected by a QPC device weakly coupled to the DQD system in the presence of a GWN environment. By analyzing the detector outcome, we study the environmental influence on the detection behavior of the system and explore the physical mechanism for the new effects induced by the GWN environment.

Figure 2 shows the average current I and the occupation of the left dot $\rho_{LL}(t)$ as functions of time t for different cases. As shown in Fig. 2, the time evolutions of the average current I and occupation of the left dot $\rho_{LL}(t)$ show good consistency in behavior. In Fig. 2(b), we find that the occupying probability $\rho_{LL}(t)$ increases with the enhancement of the decoherence rate Γ_d . The rate of the electron transfer from the left dot to the right dot slows down due to the coupling with the detector for small t , which indicates the measurement process localizes the electron in the DQD system. In Figs. 2(d) and 2(f), we find the analogous behavior of slowing down the electron transfer with the increase of the noise amplitudes in both the transverse and longitudinal directions. In a sense, the interaction with the GWN environment would also localize the system for small t . Moreover, as shown in Figs. 2(c) and 2(e), the detector current allows us to distinguish the environment parameters because the average current I would take less time to reach its stationary value with the increase of the longitudinal noise amplitude σ_Δ than that with the increase of the transverse noise amplitude σ_Ω .

Figure 3 shows the average current I and Fano factor F as a function of the level displacement Δ_0 for different decoherence rates Γ_d in the long-time limit. It is worth noting that the maximum value of the average current I presents a platform distribution for small level displacement Δ_0 , as shown in Fig. 3(a). The maxima of the average current I and Fano factor F both increase with the enhancement of the decoherence rate Γ_d . Significantly, as shown in Fig. 3(b), the Fano factor always follows the super-Poissonian distribution, which is associated with the cotunneling mechanism and the quantum coherence [49,68,69]. It is worth noting that the Fano factor changes rapidly and has a high peak value (more than 80). Due to the slow switching between different current channels connecting with the left and right reservoirs of the

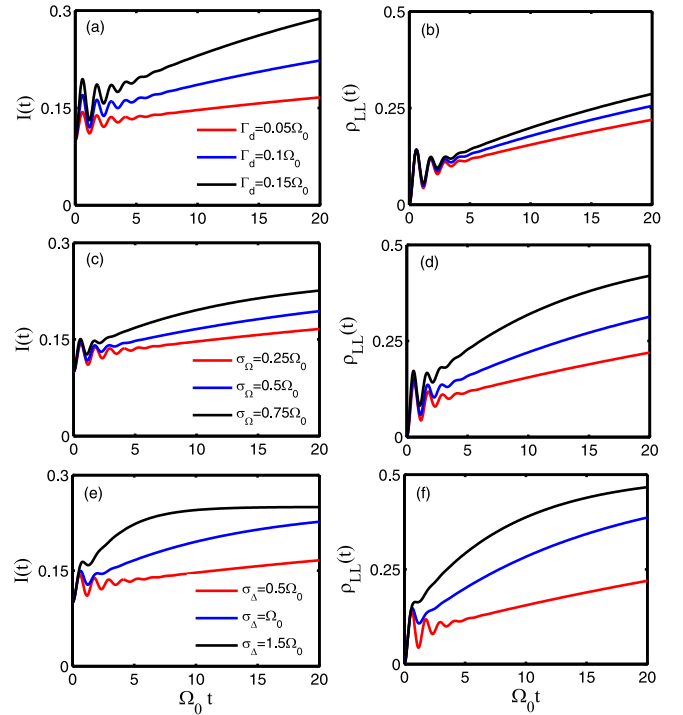


FIG. 2. Left: Time evolution of the average detector current $I(t)$ for different values of (a) the decoherence rate Γ_d caused by the QPC detector, with parameters $\sigma_\Omega = 0.25\Omega_0$ and $\sigma_\Delta = 0.5\Omega_0$, (c) the amplitude σ_Ω of the transverse noise, with parameters $\Gamma_d = 0.05\Omega_0$ and $\sigma_\Delta = 0.5\Omega_0$, and (e) the amplitude σ_Δ of the longitudinal noise, with parameters $\Gamma_d = 0.05\Omega_0$ and $\sigma_\Omega = 0.25\Omega_0$. Right: Time evolution of the occupation of the left dot $\rho_{LL}(t)$ for different values of (b) Γ_d , (d) σ_Ω , and (f) σ_Δ , where the values of the parameters are the same as in the left column. We set the electron in the right quantum dot with the initial condition $\rho_{LL}(0) = 0$ and $\rho_{RR}(0) = 1$, and the other fixed parameters are chosen to be $\Delta_0 = 2.5\Omega_0$, $\tau_\Omega = \Omega_0$, and $\tau_\Delta = \Omega_0$.

detector, which leads to a high value of the Fano factor [49], we find that the slow switching between different current channels would become more distinct because of the increase of the coupling between the detector and the DQD, which is plotted in Fig. 3(b).

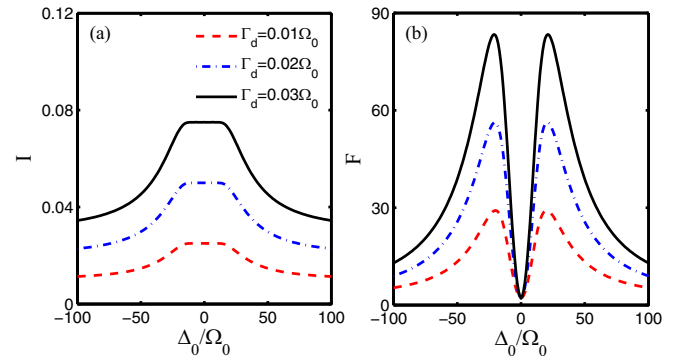


FIG. 3. (a) The average current I and (b) the Fano factor F in the long-time limit vs the level displacement Δ_0 for different values of the decoherence rate Γ_d . The noise parameters are chosen to be $\sigma_\Delta = \sigma_\Omega = 0.3\Omega_0$ and $\tau_\Omega = \tau_\Delta = \Omega_0$.

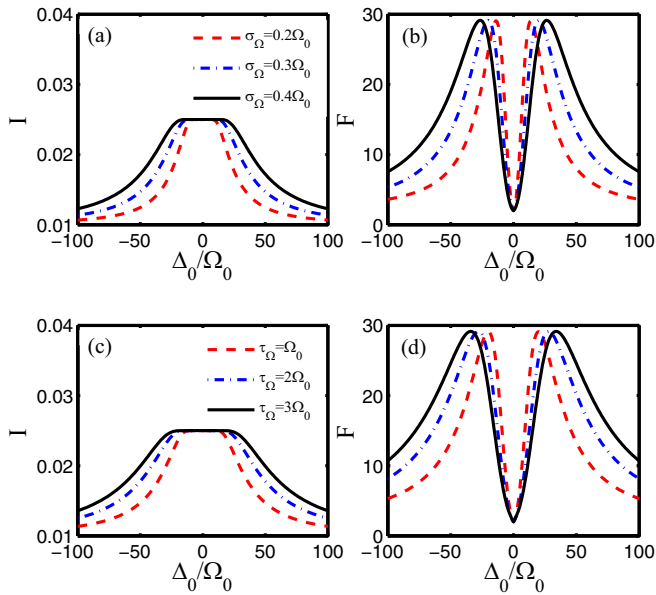


FIG. 4. (a) The average current I and (b) the Fano factor F vs the level displacement Δ_0 in the long-time limit for different values of the transverse noise amplitude σ_Ω with the transverse damping coefficient $\tau_\Omega = \Omega_0$. (c) The average current I and (d) the Fano factor F vs the level displacement Δ_0 in the long-time limit for different values of the transverse damping coefficient τ_Ω with the transverse noise amplitude $\sigma_\Omega = 0.3\Omega_0$. The other fixed parameters are the decoherence rate $\Gamma_d = 0.01\Omega_0$, the longitudinal noise amplitude $\sigma_\Delta = 0.3\Omega_0$, and the longitudinal damping coefficient $\tau_\Delta = \Omega_0$.

Figure 4 shows the influence of the transverse noise on the average current I and Fano factor F as a function of the level displacement Δ_0 for different values of the amplitude σ_Ω and damping coefficient τ_Ω . We find that both the average current I and Fano factor F show the broadening behavior with the increase of the amplitude σ_Ω and damping coefficient τ_Ω of the transverse noise. However, the maxima of the average current I and Fano factor F do not depend on the transverse noise. We find that the level displacements Δ_0 that correspond to the inflection point of the average current's platform and the two symmetrical peak points of the Fano factor are identical. This is an interesting dynamical feature to extract the noise parameters to define the environment according to the stationary detector current I and Fano factor F , which rely on the transverse noise. In the region of $|\Delta_0| < 50\Omega_0$, it is hard to accurately obtain the characteristics of the transverse noise by observing the detection current I . However, the Fano factor F is still sensitive to noise parameters in this region. The modulations of the Fano factor by noise parameters depend on the level displacement Δ_0 of different numerical ranges. When $|\Delta_0| < |\Delta_{\text{top}}|$ (Δ_{top} is the level displacement when the Fano factor reaches its maximum value and the value of $|\Delta_{\text{top}}|$ increases with the enhancements of the transverse noise parameters σ_Ω and τ_Ω), the increases of the amplitude σ_Ω and damping coefficient τ_Ω cause a reduction of the Fano factor in the long-time limit. If $|\Delta_0| > |\Delta_{\text{top}}|$, we could observe the opposite result. The sensitivity of the Fano factor at a small level displacement provides a more accurate way to acquire

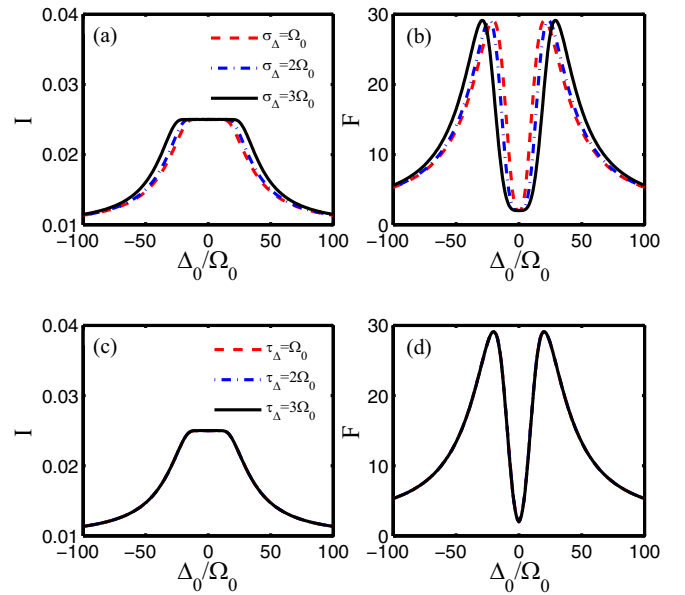


FIG. 5. (a) The average current I and (b) the Fano factor F vs the level displacement Δ_0 in the long-time limit for different values of the longitudinal noise amplitude σ_Δ with the longitudinal damping coefficient $\tau_\Delta = \Omega_0$. (c) The average current I and (d) the Fano factor F vs the level displacement Δ_0 in the long-time limit for different values of the longitudinal damping coefficient τ_Δ with the longitudinal noise amplitude $\sigma_\Delta = \Omega_0$. The other fixed parameters are the decoherence rate $\Gamma_d = 0.01\Omega_0$, the transverse noise amplitude $\sigma_\Omega = 0.3\Omega_0$, and the transverse damping coefficient $\tau_\Omega = \Omega_0$.

the environment information from the detector outcome in experiments.

Figure 5 shows the influence of the longitudinal noise on the average current I and Fano factor F as a function of the level displacement Δ_0 for different values of the amplitude σ_Δ and damping coefficient τ_Δ . Increasing the amplitude σ_Δ would cause a weak broadening behavior of the average current I and Fano factor F in Figs. 5(a) and 5(b). However, different from the strong dependence of the damping coefficient of transverse noise τ_Ω , there are no obvious distinctions from the increases of the damping coefficient τ_Δ which are plotted in Figs. 6(c) and 6(d). It is not optimal to obtain the

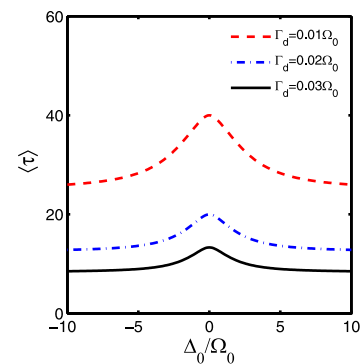


FIG. 6. The average waiting time (τ) vs the level displacement Δ_0 for different values of the decoherence rate Γ_d . The other fixed parameters are chosen to be $\sigma_\Delta = \sigma_\Omega = 0.3\Omega_0$ and $\tau_\Omega = \tau_\Delta = \Omega_0$.

environmental effects in the longitudinal direction by means of average current I and Fano factor F . We consider that one needs to calculate higher-order cumulants of electron transfer to more accurately observe the effects of longitudinal noise on the system dynamics due to the insensitivity of the average current I and Fano factor F to the longitudinal noise. The higher-order cumulant reveals additional information concerning the dynamics of electron transfer. It may contain information about the non-Gaussian behavior [70].

According to the above numerical results, we find that the value of the Fano factor gradually tends to the Poissonian limit $F = 1$ under the large level displacement Δ_0 . This dynamical feature can be attributed to the following explanation. When the level displacement Δ_0 is large (more than $100\Omega_0$), the average current I is very small, and electrons sparsely tunnel through the barrier, there is no correlation among successive tunneling events [49]. Hence, the correlations between transferred electrons would gradually disappear, which forms a Poissonian distribution ($F = 1$) as Δ_0 increases to a large value. The Poissonian limit for large Δ_0 was observed in many studies, such as the three-dot system [49], pure dephasing environment [15], strong Coulomb blockade regime [50], etc.

The average current I and Fano factor F both show symmetrical behavior. This symmetrical distribution also appeared in our previous work [15]. Based on the method of Refs. [5,13], there are no high-order terms of the coupling T_0 considered between left and right reservoirs in the detector, regardless of whether the DQD is symmetrical, and the probability of an electron occupying both sides of the DQD is equal to 0.5 when the system is in a steady state after a long period of evolution. However, if we consider the high-order terms of the coupling in the detector, the probability of electron occupancy in the DQD in the steady state should be related to the symmetry property of the DQD [42,71,72].

Figure 6 shows the average waiting time $\langle\tau\rangle$ as a function of the level displacement Δ_0 for different decoherence rates Γ_d . The electron's state is represented by the reduced density matrix $\rho_{ij}(t)$. We set the electron in the right dot at the initial time ($\rho_{RR}(0) = 1$). In the short-time limit, the electron would transfer from the right dot to the left dot, namely, $\rho_{RR}(0) = 1 \rightarrow \rho_{LL}(t_1) = 1, t_1 > 0$. We find that there is a downward shift of the average waiting time $\langle\tau\rangle$ due to the increase of the decoherence rate Γ_d . It implies the decoherence caused by the frequent measurements would promote the transfer of a single electron in the detector. This is due to the restriction of electron transfer from the right dot to the left dot in the DQD, which causes a reduction of the barrier of the detector (the electron that in the right dot is away from the detector in Fig. 1). This localized effect would become more pronounced as the decoherence rate Γ_d increases. From this dynamical property of the average waiting time $\langle\tau\rangle$, we realize that measurement enhances localization of the electron in the short-time limit.

Figure 7 shows the influence of the transverse noise on the average waiting time $\langle\tau\rangle$ as a function of the level displacement Δ_0 for different values of the amplitude σ_Ω and damping coefficient τ_Ω . It can be seen that the average waiting time $\langle\tau\rangle$ decreases with the increases of amplitude σ_Ω and damping coefficient τ_Ω . We could understand that the increasing of the amplitude σ_Ω and damping coefficient τ_Ω would slow the

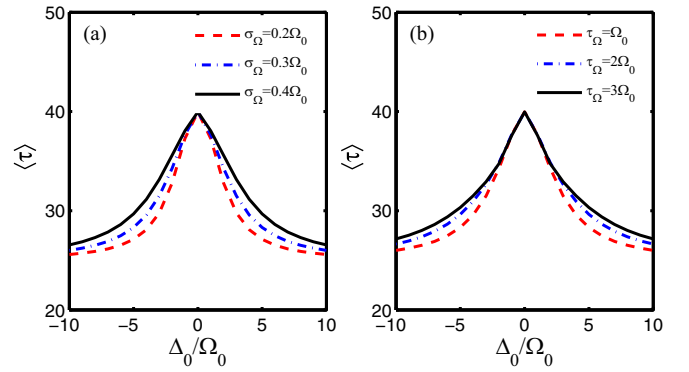


FIG. 7. (a) The average waiting time $\langle\tau\rangle$ vs the level displacement Δ_0 for different values of the transverse noise amplitude σ_Ω with the transverse damping coefficient $\tau_\Omega = \Omega_0$. (b) The average waiting time $\langle\tau\rangle$ vs the level displacement Δ_0 for different values of the transverse damping coefficient τ_Ω with the transverse noise amplitude $\sigma_\Omega = 0.3\Omega_0$. The other fixed parameters are the decoherence rate $\Gamma_d = 0.01\Omega_0$, the longitudinal noise amplitude $\sigma_\Delta = 0.3\Omega_0$, and the longitudinal damping coefficient $\tau_\Delta = \Omega_0$.

transfer of a single electron in the detector at the same level displacement. However, the transfer of a single electron in the short-time limit is not sensitive to the damping coefficient τ_Ω when the level displacement is small ($|\Delta_0| < 3\Omega_0$). It is worth noting that the peak value of the average waiting time $\langle\tau\rangle$ is not affected by the transverse noise, which is similar to the dynamics in the long-time limit in Fig. 4. Roughly speaking, we attribute this increasing behavior of the average waiting time $\langle\tau\rangle$ to the suppression of electron transfer by the transverse noise.

Figure 8 shows the influence of the longitudinal noise on the average waiting time $\langle\tau\rangle$ as a function of the level displacement Δ_0 for different values of the amplitude σ_Δ and damping coefficient τ_Δ . The presence of longitudinal noise hinders the transfer of a single electron in the detector, as

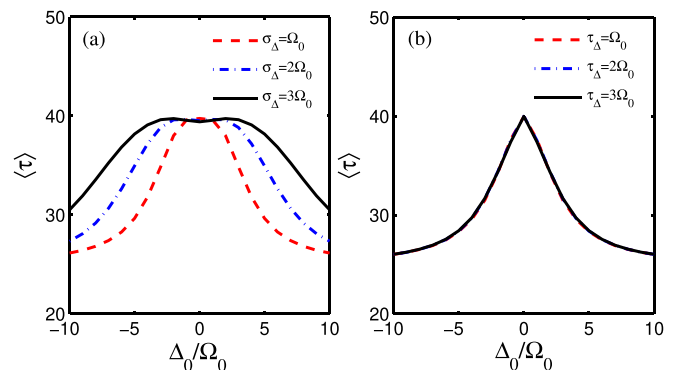


FIG. 8. (a) The average waiting time $\langle\tau\rangle$ vs the level displacement Δ_0 for different values of the longitudinal noise amplitude σ_Δ with the longitudinal damping coefficient $\tau_\Delta = \Omega_0$. (b) The average waiting time $\langle\tau\rangle$ vs the level displacement Δ_0 for different values of the longitudinal damping coefficient τ_Δ with the longitudinal noise amplitude $\sigma_\Delta = 0.3\Omega_0$. The other fixed parameters are the decoherence rate $\Gamma_d = 0.01\Omega_0$, the transverse noise amplitude $\sigma_\Omega = 0.3\Omega_0$, and the transverse damping coefficient $\tau_\Omega = \Omega_0$.

shown in Fig. 8(a). Interestingly, a weak bimodal structure appears with an increase in the noise amplitude σ_Δ . The higher amplitude of the longitudinal noise destroys the unimodal distribution of the average waiting time $\langle\tau\rangle$. This is because the fluctuation of the level displacement caused by the longitudinal noise is higher than the level displacement itself for the small Δ_0 . The dynamics in the short-time limit (average waiting time $\langle\tau\rangle$) exhibits a higher dependence on longitudinal noise amplitude than the long-time limit (average current I and Fano factor F) compared with Fig. 5. We could analyze the longitudinal noise's properties from the average waiting time $\langle\tau\rangle$ of the detector in the short-time limit. However, the change in damping coefficient τ_Δ has no obvious effect on the average waiting time $\langle\tau\rangle$ in Fig. 8(b). As discussed above, studies of the average waiting time are conducive to expanding the understanding of the dynamical behavior in a short-time limit and providing theoretical support for regulating electronic behavior.

V. CONCLUSIONS

In conclusion, we used the methods of the FCS and the additional Bloch vector to inquire into the dynamics of the weak interaction between the GWN environment and the DQD system detected by the QPC. We obtained the exact dynamical evolution equation of the system and, based on this, studied the average current, the Fano factor, and the average waiting time of the detector. It was shown that the super-Poissonian distribution of the Fano factor is related to the cotunneling and the quantum coherence. The Fano factor exhibits an enhancement associated with decoherence caused by the QPC in the long-time limit. Both the average current and Fano factor show the broadening behavior due to the coupling between the transverse noise and DQD. Moreover, the coupling of a DQD to a GWN environment usually hinders the transfer of a single electron in the detector. More dynamics can be continued to be studied in semiconductors via the innovative method of the additional Bloch vector, such as the noise spectrum and higher-order cumulants. The research on the dynamical evolution of the open system helps us to understand the decoherence process in a fluctuant environment and provides a theoretical reference for exploring the noise features in the non-Markovian dynamics.

ACKNOWLEDGMENTS

Y.Z. acknowledges the supports from National Natural Science Foundation of China (Grant No. 11974217) and Natural Science Foundation of Shandong Province (Grant No. ZR2014AM030). X.C. acknowledges the support from the National Natural Science Foundation of China (Grant No. 11947033).

APPENDIX A: DERIVATION OF THE QUANTUM MASTER EQUATION IN THE PRESENCE OF A GWN ENVIRONMENT

In this Appendix we provide the derivation of Eq. (15) in detail. We first formally derive two types of quantum master equations for the dynamical evolution of the quantum

system in the presence of environmental noise described by the Hamiltonian in Eq. (3).

1. Two types of quantum master equations

Transforming Eq. (13) into the interaction picture, the dynamical evolution equation for the stochastic density matrix reads

$$\frac{\partial}{\partial t}\rho^I(t; \delta(t)) = L_\delta^I(t)\rho^I(t; \delta(t)), \quad (\text{A1})$$

where we have defined $\rho^I(t; \delta(t)) = e^{-L_0 t} \hat{\rho}(t; \delta(t))$ and $L_\delta^I(t) = e^{-L_0 t} L_\delta(t) e^{L_0 t}$.

We define the projection operator \mathcal{P} according to [2, 17, 29]

$$\mathcal{P}\rho^I(t; \delta(t)) = \langle\rho^I(t; \delta(t))\rangle_\delta \equiv \rho^I(t). \quad (\text{A2})$$

Furthermore, we define the complementary projector $\mathcal{Q} = \mathcal{I} - \mathcal{P}$,

$$\begin{aligned} \mathcal{Q}\rho^I(t; \delta(t)) &= \rho^I(t; \delta(t)) - \langle\rho^I(t; \delta(t))\rangle_\delta \\ &\equiv \rho^I(t; \delta(t)) - \rho^I(t). \end{aligned} \quad (\text{A3})$$

The two operators have the properties $\mathcal{P}^2 = \mathcal{P}$, $\mathcal{Q}^2 = \mathcal{Q}$, and $\mathcal{P}\mathcal{Q} = \mathcal{Q}\mathcal{P} = 0$. Typically, the environmental noise is the stationary statistical property, namely, the vanishment of the odd moments,

$$\mathcal{P}L_\delta^I(t_1)L_\delta^I(t_2)\cdots L_\delta^I(t_{2n+1})\mathcal{P} = 0. \quad (\text{A4})$$

Performing the projection operators on Eq. (A1) gives

$$\begin{aligned} \frac{\partial}{\partial t}\mathcal{P}\rho^I(t; \delta(t)) &= \mathcal{P}\frac{\partial}{\partial t}\rho^I(t; \delta(t)) = \mathcal{P}L_\delta^I(t)\rho^I(t; \delta(t)), \\ \frac{\partial}{\partial t}\mathcal{Q}\rho^I(t; \delta(t)) &= \mathcal{Q}\frac{\partial}{\partial t}\rho^I(t; \delta(t)) = \mathcal{Q}L_\delta^I(t)\rho^I(t; \delta(t)). \end{aligned} \quad (\text{A5})$$

On inserting the identity $\mathcal{I} = \mathcal{P} + \mathcal{Q}$ between the Liouville operator and the density matrix and in terms of the condition in Eq. (A4), Eq. (A5) can be rewritten as

$$\begin{aligned} \frac{\partial}{\partial t}\mathcal{P}\rho^I(t; \delta(t)) &= \mathcal{P}L_\delta^I(t)\mathcal{Q}\rho^I(t; \delta(t)), \\ \frac{\partial}{\partial t}\mathcal{Q}\rho^I(t; \delta(t)) &= \mathcal{Q}L_\delta^I(t)\mathcal{P}\rho^I(t; \delta(t)) + \mathcal{Q}L_\delta^I(t)\mathcal{Q}\rho^I(t; \delta(t)). \end{aligned} \quad (\text{A6})$$

The solution of $\mathcal{Q}\rho^I(t; \delta(t))$ can be expressed as

$$\begin{aligned} \mathcal{Q}\rho^I(t; \delta(t)) &= \int_0^t dt' g(t, t') \mathcal{Q}L_\delta^I(t') \mathcal{P}\rho^I(t'; \delta(t')) \\ &\quad + g(t, 0) \mathcal{Q}\rho^I(0; \delta(0)), \end{aligned} \quad (\text{A7})$$

with the forward propagator

$$g(t, t') = \mathcal{T}_\leftarrow \exp \left[\int_{t'}^t d\tau \mathcal{Q}L_\delta^I(\tau) \right], \quad (\text{A8})$$

where \mathcal{T}_\leftarrow is the chronological time-ordering operator. The propagator $g(t, t')$ satisfies the differential equation

$$\frac{\partial}{\partial t}g(t, t') = \mathcal{Q}L_\delta^I(t)g(t, t'), \quad (\text{A9})$$

with the initial condition $g(t', t') = \mathcal{I}$.

Substituting the solution for $\mathcal{Q}\rho^I(t; \delta(t))$ into Eq. (A6) gives

$$\begin{aligned} \frac{\partial}{\partial t} \mathcal{P}\rho^I(t; \delta(t)) &= \int_0^t dt' \mathcal{P}L_\delta^I(t)g(t, t')\mathcal{Q}L_\delta^I(t')\mathcal{P}\rho^I(t'; \delta(t')) \\ &+ \mathcal{P}L_\delta^I(t)g(t, 0)\mathcal{Q}\rho^I(0; \delta(0)). \end{aligned} \quad (\text{A10})$$

When there is no initial correlation between the quantum system and environment, the initial state is given by $\mathcal{P}\rho^I(0; \delta(0)) = \rho^I(0) = \rho^I(0; \delta(0))$ and $\mathcal{Q}\rho^I(0; \delta(0)) = 0$.

Therefore, the second term on the right-hand side of Eq. (A10) vanishes; then

$$\frac{\partial}{\partial t} \mathcal{P}\rho^I(t; \delta(t)) = \int_0^t dt' \mathcal{P}L_\delta^I(t)g(t, t')\mathcal{Q}L_\delta^I(t')\mathcal{P}\rho^I(t'; \delta(t')). \quad (\text{A11})$$

Expanding the propagator $g(t, t')$ in the Dyson series

$$g(t, t') = 1 + \sum_{n=1}^{\infty} g_n(t, t'), \quad (\text{A12})$$

with $g_n(t, t') = \int_{t'}^t dt_1 \cdots \int_{t'}^{t_{n-1}} dt_n \mathcal{Q}L_\delta^I(t_1) \cdots \mathcal{Q}L_\delta^I(t_n)$, and based on the definition in Eq. (A2), we obtain the time-convolution master equation for the dynamical evolution of the quantum system

$$\frac{d}{dt} \rho^I(t) = \int_0^t dt' K(t, t') \rho^I(t'), \quad (\text{A13})$$

where the time nonlocal operator satisfies

$$\begin{aligned} &\int_0^t dt' K(t, t') \rho^I(t') \\ &= \sum_{n=2}^{\infty} \int_0^t dt_1 \cdots \int_0^{t_{n-2}} dt_{n-1} \langle L_\delta^I(t) \cdots L_\delta^I(t_{n-1}) \rangle_\delta^{\text{pc}} \rho^I(t_{n-1}), \end{aligned} \quad (\text{A14})$$

in terms of the partial cumulants

$$\begin{aligned} &\langle L_\delta^I(t) \cdots L_\delta^I(t_{n-1}) \rangle_\delta^{\text{pc}} \\ &= \sum (-1)^{q-1} \prod \langle L_\delta^I(t) \cdots \rangle_\delta \langle L_\delta^I(t_j) \cdots \rangle_\delta \cdots, \end{aligned} \quad (\text{A15})$$

with q denoting the number of averages in the term and the chronological order $t > t_1 > \cdots > t_n$ being maintained. The integro-differential equation (A13) is equivalent to that derived by Nakajima [73] and Zwanzig [74].

We further derive the time-convolutionless equation for the dynamical evolution of the quantum system. Replacing the stochastic density matrix on the right-hand side of Eq. (A10) by

$$\rho^I(t'; \delta(t')) = G(t, t') \rho^I(t; \delta(t)), \quad (\text{A16})$$

where the backward propagator is expressed as

$$G(t, t') = \mathcal{T}_\rightarrow \exp \left[- \int_{t'}^t L_\delta^I(\tau) d\tau \right], \quad (\text{A17})$$

with \mathcal{T}_\rightarrow indicating the antichronological time ordering, the solution for $\mathcal{Q}\rho^I(t; \delta(t))$ can be rewritten as

$$\mathcal{Q}\rho^I(t; \delta(t)) = \int_0^t dt' g(t, t') \mathcal{Q}L_\delta^I(t') \mathcal{P}G(t, t') \rho^I(t'; \delta(t')). \quad (\text{A18})$$

Introducing the superoperator

$$\Sigma(t) = \int_0^t dt' g(t, t') \mathcal{Q}L_\delta^I(t') \mathcal{P}G(t, t'), \quad (\text{A19})$$

Eq. (A18) can be expressed as

$$\mathcal{Q}\rho^I(t; \delta(t)) = [1 - \Sigma(t)]^{-1} \Sigma(t) \mathcal{P}\rho^I(t; \delta(t)). \quad (\text{A20})$$

Substituting the solution of $\mathcal{Q}\rho^I(t; \delta(t))$ into Eq. (A6) gives the evolution

$$\frac{\partial}{\partial t} \mathcal{P}\rho^I(t; \delta(t)) = \mathcal{P}L_\delta^I(t) [1 - \Sigma(t)]^{-1} \mathcal{P}\rho^I(t; \delta(t)). \quad (\text{A21})$$

Consequently, we obtain the time-convolutionless master equation for the dynamical evolution of the quantum system

$$\frac{d}{dt} \rho^I(t) = K(t) \rho^I(t), \quad (\text{A22})$$

where the time-local operator can be expressed as

$$K(t) = \sum_{n=1}^{\infty} \int_0^t dt_1 \cdots \int_0^{t_{n-2}} dt_{n-1} \langle L_\delta^I(t) \cdots L_\delta^I(t_{n-1}) \rangle_\delta^{\text{oc}}, \quad (\text{A23})$$

with the time-order cumulants

$$\begin{aligned} \langle L_\delta^I(t) \cdots L_\delta^I(t_{n-1}) \rangle_\delta^{\text{oc}} &= \sum (-1)^{q-1} \prod \langle L_\delta^I(t) \cdots L_\delta^I(t_i) \rangle_\delta \\ &\times \langle L_\delta^I(t_j) \cdots L_\delta^I(t_k) \rangle_\delta \cdots. \end{aligned} \quad (\text{A24})$$

Here the sum is taken over all possible divisions by keeping the chronological order $t > \cdots > t_i, t_j > \cdots > t_k$, etc.

2. Weak-coupling limit and Markovian approximation

To solve the above two types of quantum master equations exactly, we need to know the statistical characteristics of the environmental noise. In most cases, we should also make some approximations to obtain the solution.

When the coupling between the system and its environment is weak, such that the influence of the system on the environment is small, the correlation time of the environmental noise is shorter than the timescale of the quantum system. In weak-coupling limit, the evolution equation of the system can be simply truncated to second order. Correspondingly, the time-convolution quantum master equation (A13) can be reduced to

$$\frac{d}{dt} \rho^I(t) = \int_0^t dt' \langle L_\delta^I(t) L_\delta^I(t') \rangle_\delta \rho^I(t'), \quad (\text{A25})$$

and the time-convolutionless equation (A22) can be reduced to

$$\frac{d}{dt} \rho^I(t) = \int_0^t dt' \langle L_\delta^I(t) L_\delta^I(t') \rangle_\delta \rho^I(t'). \quad (\text{A26})$$

The simplified equation (A25) contains $\rho^I(t')$ in the integral, and hence, the behavior of the system depends on its past history. If we further make the assumption: $\rho^I(t)$ depends only on its present value $\rho^I(t)$. In other words, it is assumed that the system loses all memory of its past, namely, Markovian approximation. Hence, we can make the substitution $\rho^I(t') \rightarrow \rho^I(t)$, and Eq. (A25) can be further reduced to the same form as expressed in Eq. (A26).

3. Exact quantum master equation in the presence of GWN

We now derive the exact quantum master equation in the presence of GWN of the stationary OU type in both the longitudinal and transverse directions. The two Gaussian noises are fully described by their first average and second-order cumulants,

$$\begin{aligned} \langle \delta \Delta(t) \rangle_\delta &= 0, & \langle \delta \Delta(t) \delta \Delta(t') \rangle_\delta &= \sigma_\Delta^2 e^{-\tau_\Delta(t-t')}, \\ \langle \delta \Omega(t) \rangle_\delta &= 0, & \langle \delta \Omega(t) \delta \Omega(t') \rangle_\delta &= \sigma_\Omega^2 e^{-\tau_\Omega(t-t')}, \end{aligned} \quad (\text{A27})$$

and their higher time-order cumulants vanish [17]:

$$\begin{aligned} \langle \delta \Delta(t) \delta \Delta(t_1) \cdots \delta \Delta(t_{n-1}) \rangle_\delta^{\text{oc}} &= 0, \\ \langle \delta \Omega(t) \delta \Omega(t_1) \cdots \delta \Omega(t_{n-1}) \rangle_\delta^{\text{oc}} &= 0 \end{aligned} \quad (\text{A28})$$

for $n \geq 3$. We further assume the longitudinal and transverse noises are independent of each other:

$$\langle \delta \Delta(t) \delta \Omega(t) \rangle_\delta = \langle \delta \Delta(t) \rangle_\delta \langle \delta \Omega(t) \rangle_\delta = 0. \quad (\text{A29})$$

In terms of the above properties of the noise, we can find for $n \geq 3$

$$\langle L_\delta^I(t) \cdots L_\delta^I(t_{n-1}) \rangle_\delta^{\text{oc}} = 0. \quad (\text{A30})$$

As a consequence, the second-order time-convolutionless equation describes the exact dynamical evolution of the system in the presence of Gaussian white noise,

$$\frac{d}{dt} \rho^I(t) = \int_0^t dt' \langle L_\delta^I(t) L_\delta^I(t') \rangle_\delta \rho^I(t'). \quad (\text{A31})$$

Transforming Eq. (A31) back to Schrödinger picture, the dynamical evolution of the system satisfies the quantum master equation

$$\frac{d}{dt} \rho(t) = L_0 \rho(t) + \int_0^t dt' \langle L_\delta(t) e^{L_0(t-t')} L_\delta(t') \rangle_\delta e^{-L_0(t-t')} \rho(t'). \quad (\text{A32})$$

APPENDIX B: DERIVATION OF EVOLUTION OF THE ELEMENTS OF THE REDUCED DENSITY MATRIX

In this Appendix we provide the derivation of Eq. (B7) in detail. In terms of the column vector representation

for the reduced density matrix of the system $\rho(t) = [\rho_{LL}(t), \rho_{RR}(t), \rho_{RL}(t), \rho_{LR}(t)]^\dagger$, to obtain the expression of the evolution of the elements of the reduced density matrix in Eq. (15) we should express the matrix e^{L_0} as

$$e^{L_0} = S^\dagger e^{L'_0} S, \quad (\text{B1})$$

based on the diagonalization of the matrix L_0 as

$$L'_0 = S L_0 S^\dagger = \begin{pmatrix} 0 & 0 & 0 & 0 \\ 0 & 0 & 0 & 0 \\ 0 & 0 & -i\Omega_L & 0 \\ 0 & 0 & 0 & i\Omega_L \end{pmatrix}, \quad (\text{B2})$$

where S is the transformation matrix

$$S = \begin{pmatrix} \frac{1}{\sqrt{2}} & \frac{1}{\sqrt{2}} & 0 & 0 \\ \frac{\Delta_0}{\sqrt{2}\Omega_L} & -\frac{\Delta_0}{\sqrt{2}\Omega_L} & \frac{\Omega_0}{\sqrt{2}\Omega_L} & \frac{\Omega_0}{\sqrt{2}\Omega_L} \\ -\frac{\Omega}{2\Omega_L} & \frac{\Omega}{2\Omega_L} & \frac{\Omega_L + \Delta_0}{2\Omega_L} & -\frac{\Omega_L - \Delta_0}{2\Omega_L} \\ -\frac{\Omega}{2\Omega_L} & \frac{\Omega}{2\Omega_L} & -\frac{\Omega_L - \Delta_0}{2\Omega_L} & \frac{\Omega_L + \Delta_0}{2\Omega_L} \end{pmatrix}. \quad (\text{B3})$$

The superoperator $L_\delta(t)$ that describes the fluctuation effect of the environmental noise on the density matrix can be written as

$$L_\delta(t) = -i \frac{\delta \Delta(t)}{2} L_{\sigma_z} - i \frac{\delta \Omega(t)}{2} L_{\sigma_x}, \quad (\text{B4})$$

where we use the definitions $L_{\sigma_x} \rho(t) = [\sigma_x, \rho(t)]$ and $L_{\sigma_z} \rho(t) = [\sigma_z, \rho(t)]$ with the superoperators

$$\begin{aligned} L_{\sigma_z} &= \begin{pmatrix} 0 & 0 & 0 & 0 \\ 0 & 0 & 0 & 0 \\ 0 & 0 & 2 & 0 \\ 0 & 0 & 0 & -2 \end{pmatrix}, \\ L_{\sigma_x} &= \begin{pmatrix} 0 & 0 & -1 & 1 \\ 0 & 0 & 1 & -1 \\ -1 & 1 & 0 & 0 \\ 1 & -1 & 0 & 0 \end{pmatrix}. \end{aligned} \quad (\text{B5})$$

Because the longitudinal and transverse noises are independent of each other, the second term on the right-hand side of Eq. (15) satisfies

$$\begin{aligned} \int_0^t dt' \langle L_\delta(t) e^{L_0(t-t')} L_\delta(t') \rangle_\delta e^{-L_0(t-t')} \rho(t) &= -\frac{1}{4} \int_0^t dt' \langle \delta \Delta(t) \delta \Delta(t') \rangle L_{\sigma_z} S^\dagger e^{L'_0(t-t')} S L_{\sigma_z} e^{-L_0(t-t')} \rho(t) \\ &\quad - \frac{1}{4} \int_0^t dt' \langle \delta \Omega(t) \delta \Omega(t') \rangle L_{\sigma_x} S^\dagger e^{L'_0(t-t')} S L_{\sigma_x} e^{-L_0(t-t')} \rho(t). \end{aligned} \quad (\text{B6})$$

In terms of the correlation functions of the longitudinal and transverse OU-type GWN defined in Eq. (12) and the superoperators defined above, we obtain the expression of the evolution of the elements of the reduced density matrix as

$$\begin{aligned} \dot{\rho}_{LL}(t) &= -\Omega_0 \left\{ \frac{i}{2} + \frac{\Delta_0 \sigma_\Omega^2}{2\Omega_L^2} \left[\frac{1}{(\tau_\Omega^2 + \Omega_L^2)} [\tau_\Omega - e^{-\tau_\Omega t} \tau_\Omega \cos(\Omega_L t) + \Omega_L e^{-\tau_\Omega t} \sin(\Omega_L t)] - \frac{(1 - e^{-\tau_\Omega t})}{\tau_\Omega} \right] \right\} \rho_{RL}(t) \\ &\quad + \Omega_0 \left\{ \frac{i}{2} - \frac{\Delta_0 \sigma_\Omega^2}{2\Omega_L^2} \left[\frac{1}{(\tau_\Omega^2 + \Omega_L^2)} [\tau_\Omega - e^{-\tau_\Omega t} \tau_\Omega \cos(\Omega_L t) + \Omega_L e^{-\tau_\Omega t} \sin(\Omega_L t)] + \frac{(1 - e^{-\tau_\Omega t})}{\tau_\Omega} \right] \right\} \rho_{LR}(t) \\ &\quad - \frac{\sigma_\Omega^2}{2\Omega_L^2} \left[\frac{\Delta_0^2}{(\tau_\Omega^2 + \Omega_L^2)} [\tau_\Omega - e^{-\tau_\Omega t} \tau_\Omega \cos(\Omega_L t) + \Omega_L e^{-\tau_\Omega t} \sin(\Omega_L t)] + \frac{\Omega_0^2}{\tau_\Omega} (1 - e^{-\tau_\Omega t}) \right] [\rho_{LL}(t) - \rho_{RR}(t)], \end{aligned}$$

$$\begin{aligned}
\dot{\rho}_{RL}(t) = & \left[-i\frac{\Omega_0}{2} - i\frac{\Omega_0\sigma_\Delta^2}{2\Omega_L(\tau_\Delta^2 + \Omega_L^2)} [\Omega_L - \tau_\Delta e^{-\tau_\Delta t} \sin(\Omega_L t) - \Omega_L e^{-\tau_\Delta t} \cos(\Omega_L t)] \right. \\
& - \frac{\Omega_0\Delta_0\sigma_\Delta^2}{2\Omega_L(\tau_\Delta^2 + \Omega_L^2)} [\tau_\Delta - e^{-\tau_\Delta t} \tau_\Delta \cos(\Omega_L t) + e^{-\tau_\Delta t} \Omega_L \sin(\Omega_L t)] + \frac{\Delta_0\Omega_0\sigma_\Delta^2}{2\Omega_L^2\tau_\Delta} (1 - e^{-\tau_\Delta t}) \left. \right] [\rho_{LL}(t) - \rho_{RR}(t)] \\
& - \left[\frac{\Omega_0^2\sigma_\Omega^2}{2\tau_\Omega\Omega_L^2} (1 - e^{-\tau_\Omega t}) + \frac{\Delta_0^2\sigma_\Omega^2}{2\Omega_L^2(\tau_\Omega^2 + \Omega_L^2)} [\tau_\Omega - e^{-\tau_\Omega t} \tau_\Omega \cos(\Omega_L t) + \Omega_L e^{-\tau_\Omega t} \sin(\Omega_L t)] \right] [\rho_{RL}(t) - \rho_{LR}(t)] \\
& + \frac{i\Delta_0\sigma_\Omega^2}{2\Omega_L(\tau_\Omega^2 + \Omega_L^2)} [\Omega_L - \tau_\Omega e^{-\tau_\Omega t} \sin(\Omega_L t) - \Omega_L e^{-\tau_\Omega t} \cos(\Omega_L t)] [\rho_{RL}(t) + \rho_{LR}(t)] \\
& + \left[i\Delta_0 - \frac{\Delta_0^2\sigma_\Delta^2}{\Omega_L^2\tau_\Delta} (1 - e^{-\tau_\Delta t}) - \frac{\Omega_0^2\sigma_\Delta^2}{\Omega_L^2(\tau_\Delta^2 + \Omega_L^2)} [\tau_\Delta - e^{-\tau_\Delta t} \tau_\Delta \cos(\Omega_L t) + e^{-\tau_\Delta t} \Omega_L \sin(\Omega_L t)] \right] \rho_{RL}(t). \quad (B7)
\end{aligned}$$

-
- [1] M. A. Nielsen and I. L. Chuang, *Quantum Computation and Quantum Information* (Cambridge University Press, Cambridge, 2000).
- [2] H. P. Breuer and F. Petruccione, *The Theory of Open Quantum Systems* (Oxford University Press, New York, 2002).
- [3] G. S. Engel, T. R. Calhoun, E. L. Read, T.-K. Ahn, T. Mančal, Y.-C. Cheng, R. E. Blankenship, and G. R. Fleming, *Nature (London)* **446**, 782 (2007).
- [4] S. A. Gurvitz and Y. S. Prager, *Phys. Rev. B* **53**, 15932 (1996).
- [5] S. A. Gurvitz, *Phys. Rev. B* **56**, 15215 (1997).
- [6] A. N. Korotkov and D. V. Averin, *Phys. Rev. B* **64**, 165310 (2001).
- [7] D. Mozyrsky, L. Fedichkin, S. A. Gurvitz, and G. P. Berman, *Phys. Rev. B* **66**, 161313(R) (2002).
- [8] G. B. Serapiglia, E. Paspalakis, C. Sirtori, K. L. Vodopyanov, and C. C. Phillips, *Phys. Rev. Lett.* **84**, 1019 (2000).
- [9] I. Marvian and R. W. Spekkens, *Nat. Commun.* **5**, 3821 (2014).
- [10] C. J. Myatt, B. E. King, Q. A. Turchette, C. A. Sackett, D. Kielpinski, W. M. Itano, C. Monroe, and D. J. Wineland, *Nature (London)* **403**, 269 (2000).
- [11] S. Ballmann, R. Härtle, P. B. Coto, M. Elbing, M. Mayor, M. R. Bryce, M. Thoss, and H. B. Weber, *Phys. Rev. Lett.* **109**, 056801 (2012).
- [12] J.-L. Orgiazzi, C. Deng, D. Layden, R. Marchildon, F. Kitapli, F. Shen, M. Bal, F. R. Ong, and A. Lupascu, *Phys. Rev. B* **93**, 104518 (2016).
- [13] S. A. Gurvitz, L. Fedichkin, D. Mozyrsky, and G. P. Berman, *Phys. Rev. Lett.* **91**, 066801 (2003).
- [14] N. Brunner and C. Simon, *Phys. Rev. Lett.* **105**, 010405 (2010).
- [15] L. Kang, Y. Zhang, X. Xu, and X. Tang, *Phys. Rev. B* **96**, 235417 (2017).
- [16] Y.-T. Wang, J.-S. Tang, Z.-Y. Wei, S. Yu, Z.-J. Ke, X.-Y. Xu, C.-F. Li, and G.-C. Guo, *Phys. Rev. Lett.* **118**, 020403 (2017).
- [17] F. Shibata and T. Arimitsu, *J. Phys. Soc. Jpn.* **49**, 891 (1980).
- [18] H.-P. Breuer, E.-M. Laine, and J. Piilo, *Phys. Rev. Lett.* **103**, 210401 (2009).
- [19] A. Rivas, S. F. Huelga, and M. B. Plenio, *Phys. Rev. Lett.* **105**, 050403 (2010).
- [20] W.-M. Zhang, P.-Y. Lo, H.-N. Xiong, M. W.-Y. Tu, and F. Nori, *Phys. Rev. Lett.* **109**, 170402 (2012).
- [21] F. F. Fanchini, G. Karpat, B. Çakmak, L. K. Castelano, G. H. Aguilar, O. J. Fariñas, S. P. Walborn, P. H. Souto Ribeiro, and M. C. de Oliveira, *Phys. Rev. Lett.* **112**, 210402 (2014).
- [22] H.-P. Breuer, E.-M. Laine, J. Piilo, and B. Vacchini, *Rev. Mod. Phys.* **88**, 021002 (2016).
- [23] I. de Vega and D. Alonso, *Rev. Mod. Phys.* **89**, 015001 (2017).
- [24] M. Ban, S. Kitajima, and F. Shibata, *Phys. Rev. A* **82**, 022111 (2010).
- [25] X. Cai and Y. Zheng, *Phys. Rev. A* **94**, 042110 (2016).
- [26] X. Cai and Y. Zheng, *Phys. Rev. A* **95**, 052104 (2017).
- [27] X. Cai and Y. Zheng, *J. Chem. Phys.* **149**, 094107 (2018).
- [28] X. Cai, R. Meng, Y. Zhang, and L. Wang, *Europhys. Lett.* **125**, 30007 (2019).
- [29] X. Cai, *Entropy* **21**, 1040 (2019).
- [30] X. Cai, *Sci. Rep.* **10**, 88 (2020).
- [31] M. W. Y. Tu and W.-M. Zhang, *Phys. Rev. B* **78**, 235311 (2008).
- [32] A. Braggio, J. König, and R. Fazio, *Phys. Rev. Lett.* **96**, 026805 (2006).
- [33] C. Flindt, T. Novotný, A. Braggio, M. Sassetti, and A.-P. Jauho, *Phys. Rev. Lett.* **100**, 150601 (2008).
- [34] C. Flindt, T. Novotný, A. Braggio, and A.-P. Jauho, *Phys. Rev. B* **82**, 155407 (2010).
- [35] K. H. Thomas and C. Flindt, *Phys. Rev. B* **87**, 121405(R) (2013).
- [36] Y. Yan, *Phys. Rev. A* **58**, 2721 (1998).
- [37] X.-Q. Li, P. Cui, and Y. J. Yan, *Phys. Rev. Lett.* **94**, 066803 (2005).
- [38] G. P. Zhao, Y. H. Zhang, X. J. Cai, X. L. Xu, and L. S. Kang, *Phys. E (Amsterdam, Neth.)* **84**, 10 (2016).
- [39] Y. Zhang, L. Kang, X. Xu, X. Tang, H. Li, and X. Cai, *Mod. Phys. Lett. B* **31**, 1730004 (2017).
- [40] X.-Q. Li, J. Luo, Y.-G. Yang, P. Cui, and Y. J. Yan, *Phys. Rev. B* **71**, 205304 (2005).
- [41] U. Hartmann and F. K. Wilhelm, *Phys. Rev. B* **75**, 165308 (2007).
- [42] S.-H. Ouyang, C.-H. Lam, and J. Q. You, *Phys. Rev. B* **81**, 075301 (2010).
- [43] R. Sánchez, S. Kohler, P. Hänggi, and G. Platero, *Phys. Rev. B* **77**, 035409 (2008).

- [44] A. Stockklauser, P. Scarlino, J. V. Koski, S. Gasparinetti, C. K. Andersen, C. Reichl, W. Wegscheider, T. Ihn, K. Ensslin, and A. Wallraff, *Phys. Rev. X* **7**, 011030 (2017).
- [45] T. R. Hartke, Y.-Y. Liu, M. J. Gullans, and J. R. Petta, *Phys. Rev. Lett.* **120**, 097701 (2018).
- [46] R. Sánchez, G. Platero, and T. Brandes, *Phys. Rev. Lett.* **98**, 146805 (2007).
- [47] C. Xu and M. G. Vavilov, *Phys. Rev. B* **88**, 195307 (2013).
- [48] B. Liu, F.-Y. Zhang, J. Song, and H.-S. Song, *Sci. Rep.* **5**, 11726 (2015).
- [49] C. Flindt, T. Novotný, and A.-P. Jauho, *Phys. Rev. B* **70**, 205334 (2004).
- [50] G. Kießlich, E. Schöll, T. Brandes, F. Hohls, and R. J. Haug, *Phys. Rev. Lett.* **99**, 206602 (2007).
- [51] G. Kießlich, A. Wacker, and E. Schöll, *Phys. Rev. B* **68**, 125320 (2003).
- [52] R. Aguado and L. P. Kouwenhoven, *Phys. Rev. Lett.* **84**, 1986 (2000).
- [53] M. K. Olsen and J. F. Corney, *Phys. Rev. A* **87**, 033839 (2013).
- [54] M. Albert, C. Flindt, and M. Büttiker, *Phys. Rev. Lett.* **107**, 086805 (2011).
- [55] M. Albert, G. Haack, C. Flindt, and M. Büttiker, *Phys. Rev. Lett.* **108**, 186806 (2012).
- [56] S. A. Gurvitz and D. Mozysky, *Phys. Rev. B* **77**, 075325 (2008).
- [57] J.-M. Zhang, J. Jing, L.-G. Wang, and S.-Y. Zhu, *Phys. Rev. A* **98**, 012135 (2018).
- [58] F. C. Lombardo and P. I. Villar, *Phys. Rev. A* **89**, 012110 (2014).
- [59] J. Bylander, S. Gustavsson, F. Yan, F. Yoshihara, K. Harrabi, G. Fitch, D. G. Cory, Y. Nakamura, J.-S. Tsai, and W. D. Oliver, *Nat. Phys.* **7**, 565 (2011).
- [60] X.-L. Zhen, F.-H. Zhang, G. Feng, H. Li, and G.-L. Long, *Phys. Rev. A* **93**, 022304 (2016).
- [61] A. Chenu, M. Beau, J. Cao, and A. del Campo, *Phys. Rev. Lett.* **118**, 140403 (2017).
- [62] P. W. Anderson, *J. Phys. Soc. Jpn.* **9**, 316 (1954).
- [63] R. Kubo, *J. Phys. Soc. Jpn.* **9**, 935 (1954).
- [64] R. Kubo, M. Toda, and N. Hashitsume, *Statistical Physics II: Nonequilibrium Statistical Mechanics* (Springer, Berlin, 1985).
- [65] R. Zwanzig, *Nonequilibrium Statistical Mechanics* (Oxford University Press, Oxford, 2001).
- [66] C. Emary, D. Marcos, R. Aguado, and T. Brandes, *Phys. Rev. B* **76**, 161404(R) (2007).
- [67] Y. Zheng and F. L. H. Brown, *Phys. Rev. Lett.* **90**, 238305 (2003).
- [68] E. V. Sukhorukov, G. Burkard, and D. Loss, *Phys. Rev. B* **63**, 125315 (2001).
- [69] A. Thielmann, M. H. Hettler, J. König, and G. Schön, *Phys. Rev. Lett.* **95**, 146806 (2005).
- [70] N. V. Kampen, *Stochastic Processes in Physics and Chemistry* (North-Holland, Amsterdam, 2007).
- [71] X.-Q. Li, W.-K. Zhang, P. Cui, J. Shao, Z. Ma, and Y. J. Yan, *Phys. Rev. B* **69**, 085315 (2004).
- [72] S.-H. Ouyang, C.-H. Lam, and J. Q. You, *J. Phys.: Condens. Matter* **18**, 11551 (2006).
- [73] S. Nakajima, *Prog. Theor. Phys.* **20**, 948 (1958).
- [74] R. Zwanzig, *J. Chem. Phys.* **33**, 1338 (1960).